US009513166B2

(12) **United States Patent**
Marchant et al.

(10) **Patent No.: US 9,513,166 B2**
(45) **Date of Patent: Dec. 6, 2016**

(54) SPLIT FIELD SPECTRAL IMAGER

(71) Applicants: **Alan B. Marchant**, Hyrum, UT (US); **Stephanie W. Sullivan**, Cusick, WA (US)

(72) Inventors: **Alan B. Marchant**, Hyrum, UT (US); **Stephanie W. Sullivan**, Cusick, WA (US)

(73) Assignee: **Utah State University Research Foundation**, North Logan, UT (US)

(*) Notice: Subject to any disclaimer, the term of this patent is extended or adjusted under 35 U.S.C. 154(b) by 86 days.

(21) Appl. No.: **14/333,150**

(22) Filed: **Jul. 16, 2014**

(65) **Prior Publication Data**

US 2015/0022809 A1 Jan. 22, 2015

Related U.S. Application Data

(60) Provisional application No. 61/846,986, filed on Jul. 16, 2013.

(51) **Int. Cl.**
G01J 3/45 (2006.01)
G01J 3/28 (2006.01)
G01J 3/26 (2006.01)

(52) **U.S. Cl.**
CPC ***G01J 3/2823*** (2013.01); ***G01J 3/26*** (2013.01)

(58) **Field of Classification Search**
CPC G01J 3/2823; G01J 3/26; G01J 2003/2879; G01W 1/10; G01W 2001/003
USPC 356/456
See application file for complete search history.

(56) **References Cited**

U.S. PATENT DOCUMENTS

5,325,175 A 6/1994 Mocker et al.
5,696,579 A 12/1997 Johnson
6,351,307 B1 2/2002 Erskine
2003/0184748 A1* 10/2003 McCarthy G01J 3/2823 356/328
2007/0276598 A1* 11/2007 Tillotson G01S 19/14 342/357.52
2010/0102203 A1 4/2010 Grund
2011/0164783 A1 7/2011 Hays et al.

FOREIGN PATENT DOCUMENTS

WO 9815798 4/1998

OTHER PUBLICATIONS

Ucar, Exosphere—overview, 2011, Online: http://scied.ucar.edu/shortcontent/exosphere-overview.

(Continued)

Primary Examiner — Tarifur Chowdhury
Assistant Examiner — Jonathon Cook

(57) ABSTRACT

An apparatus for spectroscopic Doppler imaging comprises collection and focusing optics, a field splitter configured to form a composite image from multiple fields of view, and a Fabry-Perot etalon configured to spatially modulate the incoming light in order to analyze the spectral content of the light from spatially resolved regions of a scene. Methods for Doppler imaging of a scene comprise split-field imagery and scene scanning techniques to create a spatially resolved spectral profile spectra of a scene, useful for measuring and profiling wind vectors and temperatures within the scene.

9 Claims, 7 Drawing Sheets

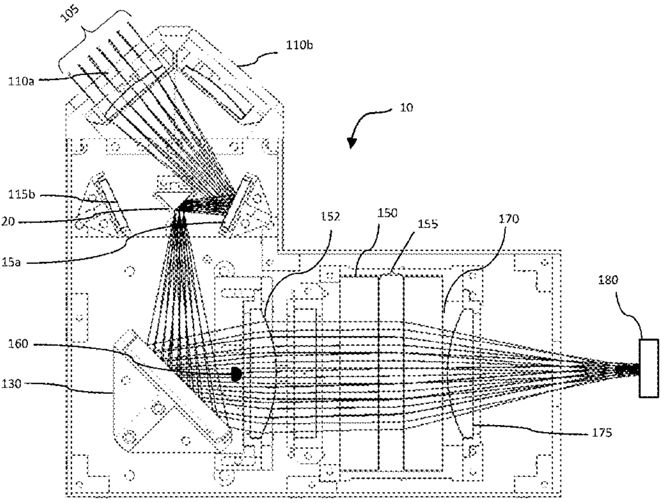

(56) **References Cited**

OTHER PUBLICATIONS

A. Christensen et al., Observations of Molecular Oxygen Atmospheric Band Emission in the Thermosphere Us-ing the Near Infrared Spectrometer on the iss/raids Experiment, Journal of Geophysical Research, Apr. 24, 2012, vol. 117, iss. A4.

V. Krassovsky et al., Atlas of the Airglow Spectrum 3000-12400a, Planetary and Space Science, 1962, p. 883-915, vol. 9, iss. 12.

G. Shepherd et al., WINDII, the Wind Imaging Interferometer on the Upper Atmosphere Research Satellite, Journal of Geophysical Research, Jun. 20, 1993, p. 10725-10750, vol. 98, iss. D6.

P. Hays et al., The High-resolution Doppler Imager on the Upper Atmosphere Research Satellite, Journal of Geophysical Research, Jun. 20, 1993, p. 10713-10723, vol. 98, iss. D6.

University of Michigan, The High Resolution Doppler Imager, http://hrdi.engin.umich.edu/.

B. Webster, 500-Mile Footprint for Debris, 2011, online: http://www.washingtonpost.com/national/health-science/500-mile-footprint-for-debris/2011/09/18/gIQAuUjedK_graphic.html.

Canadian Space Agency, OSIRIS at the Forefront of the Study of Ozone Depletion, 2001, online: http://www.asc-csa.gc.ca/eng/satellites/odin.asp.

GATS Inc., Facts, 2007, online: http://www.asc-csa.gc.ca/eng/satellites/odin.asp.

University of Michigan, TIDI Team, Data Quality and Validation, online: http://tidi.engin.umich.edu/html/go?scripts/quality_validation.pl&menu_home.html.

T. Killeen et al., TIMED Doppler Interferometer: Overview and Recent Results, Journal of Geophysical Research, 2006, vol. 111, iss. A10.

NASA, NASA Image: S129E009592, 2012, online: http://www.nasa.gov/mission_pages/station/research/experiments/689.html.

Pumpkin Inc., CubeSat Kit, 2012, online: http://www.cubesatkit.com/.

S.C. Barden et al., Volume-Phase Holographic Gratings and Their Potential for Astronomical Applications, 1998, p. 866-876, vol. 3355.

Semiconductor Components Industries LLC, HAS2 Image Sensor, 2012, online:http://www.onsemi.com/pub_link/Collateral/NOIH2SM1000A-D.PDF.

C. Englert et al., Initial Gound-based Thermospheric Wind Measurements Using Doppler Asymmetric Spatial Heterodyne Spectroscopy (DASH), Optics Express, 2010, p. 27416-27430, vol. 18, iss. 26.

P. Sheese et al., Temperatures in the Upper Mesosphere and Lower Thermosphere from OSIRIS Observations of O2A-band Emission Spectra, Canadian Journal of Physics, 2010, p. 919-925, vol. 88.

* cited by examiner

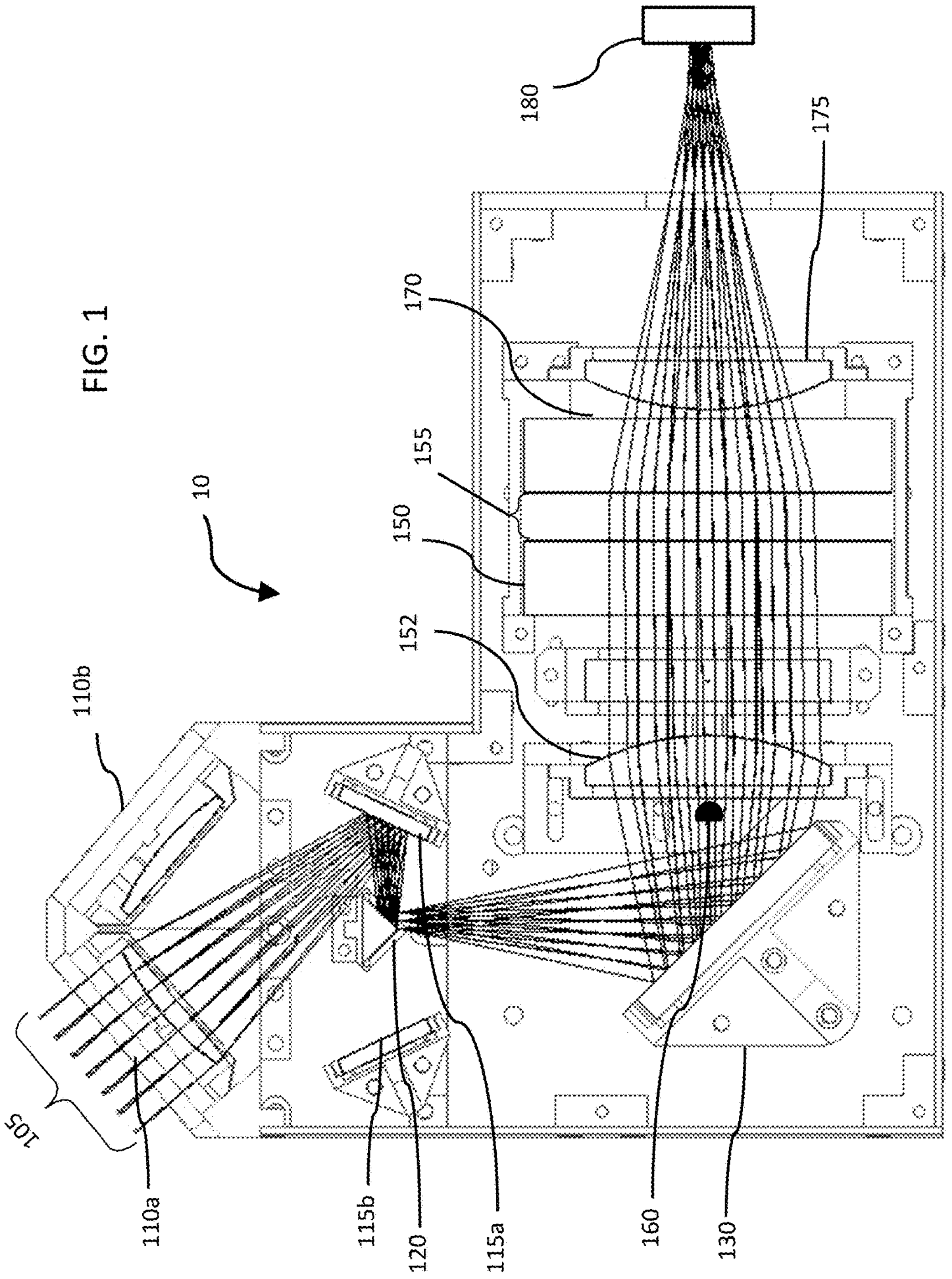

FIG. 1

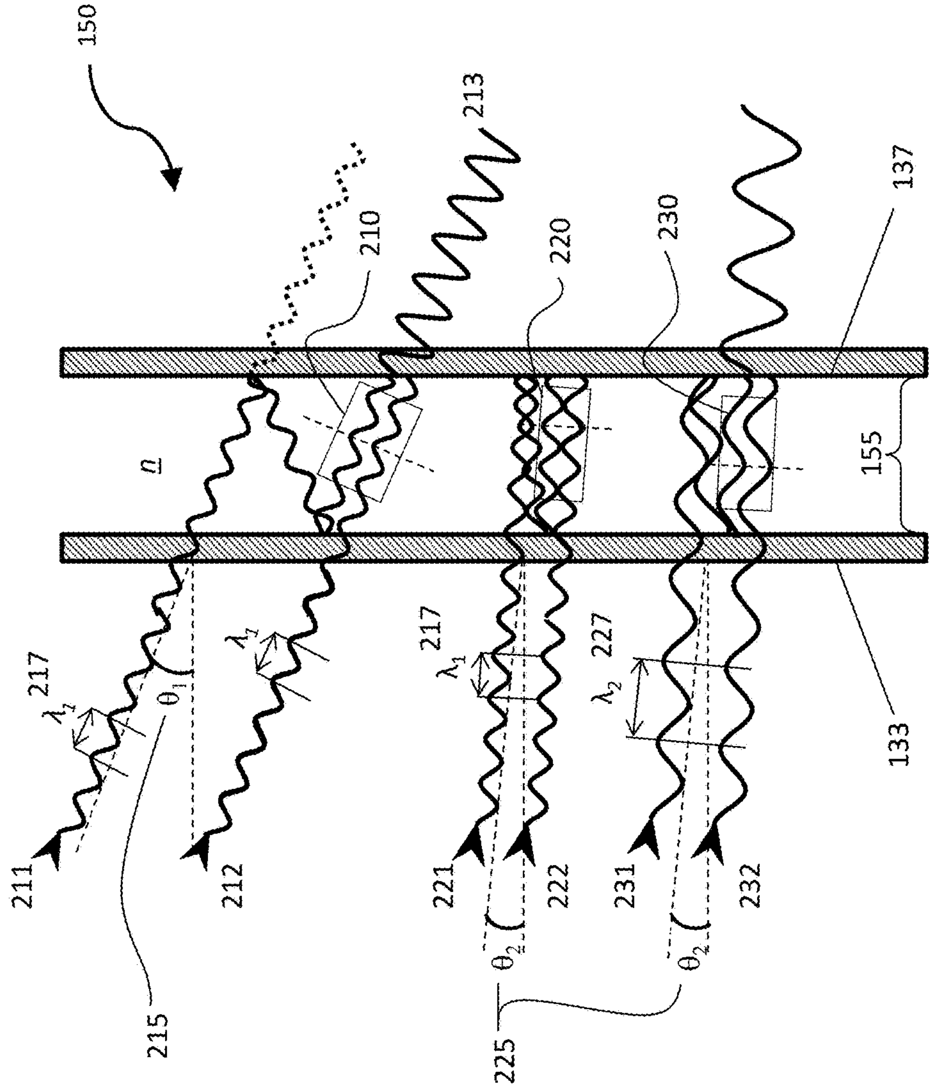
150
213
210
220
230
137
n
155
217
λ_1
λ_2
θ_1
211
212
215
217
λ_1
227
λ_2
221
222
231
232
θ_2
θ_2
225
133

FIG. 2

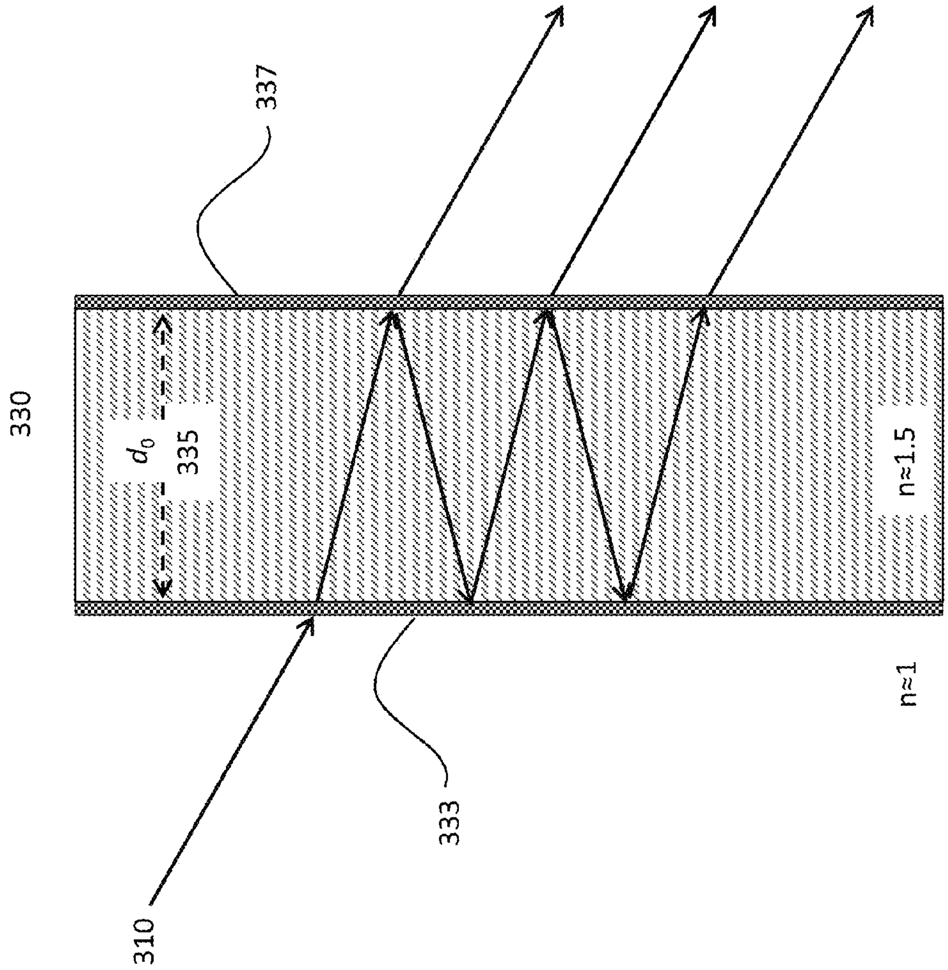

FIG. 3

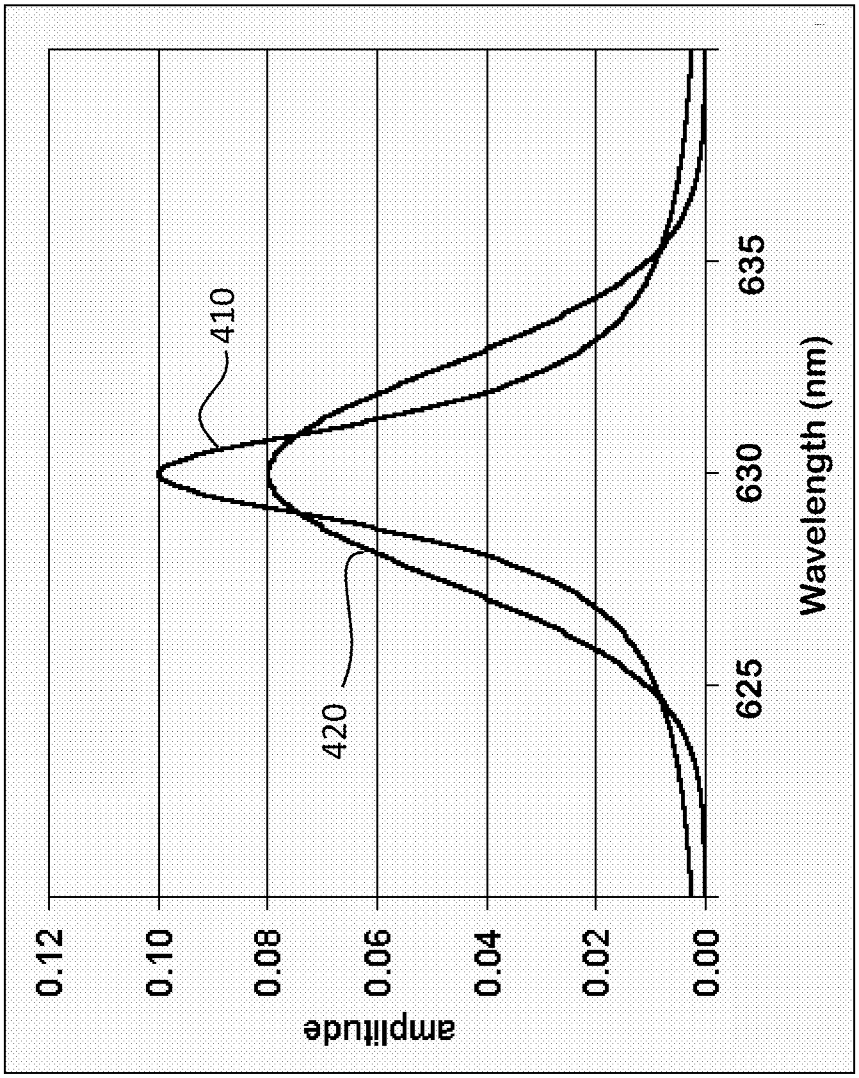
amplitude
0.12
0.10
0.08
0.06
0.04
0.02
0.00
625
630
635
Wavelength (nm)
410
420

FIG. 4

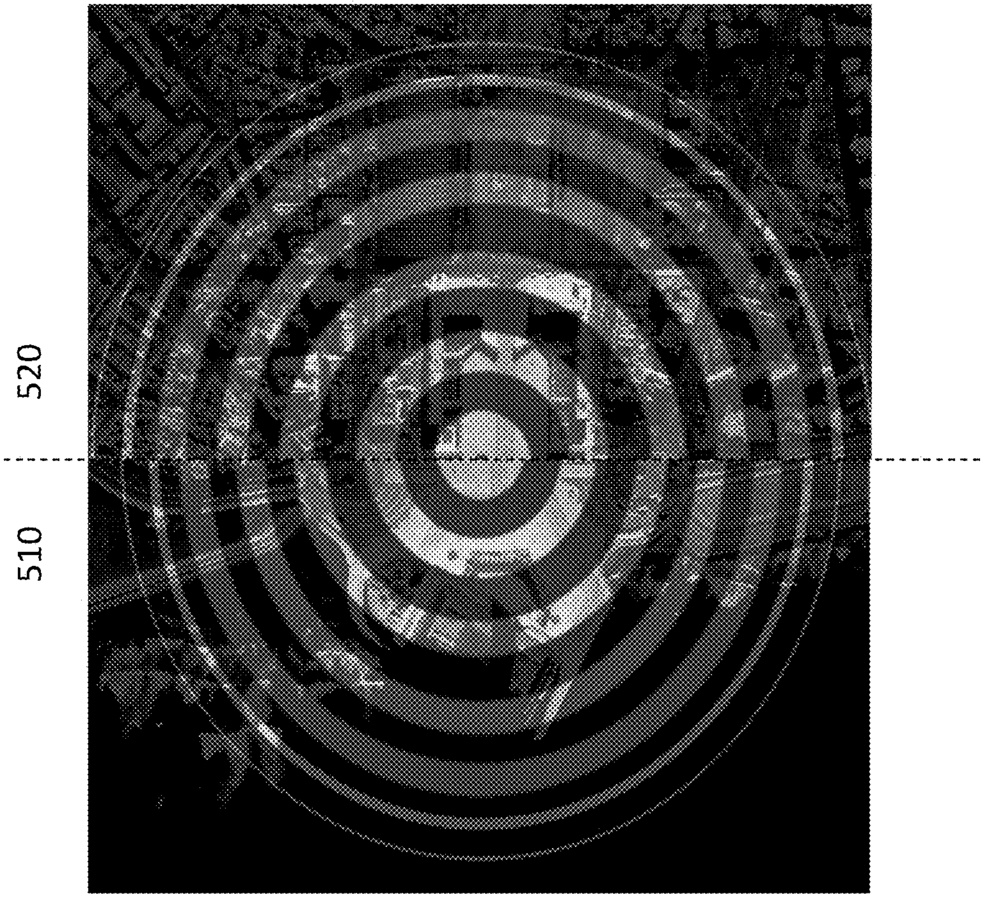

FIG. 5

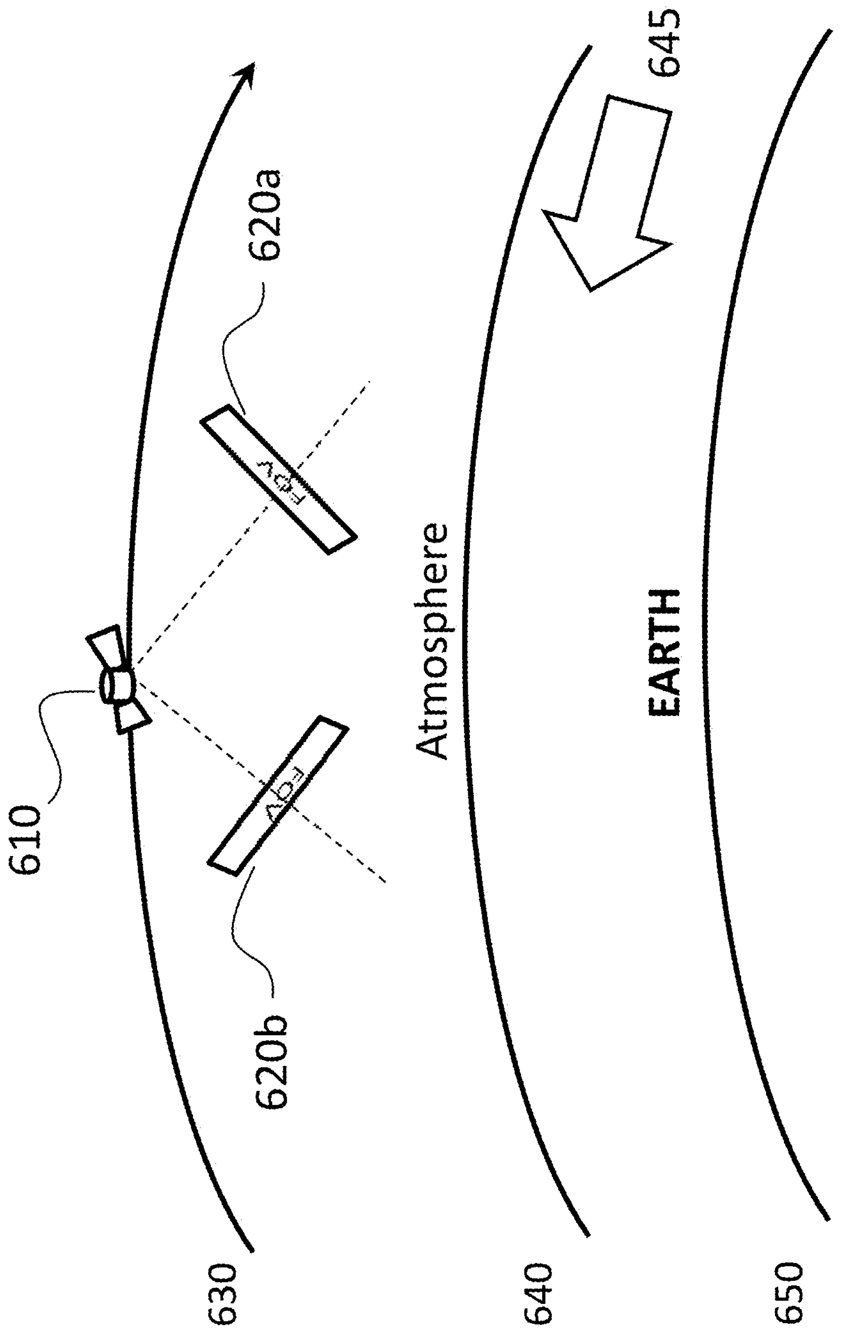

FIG. 6

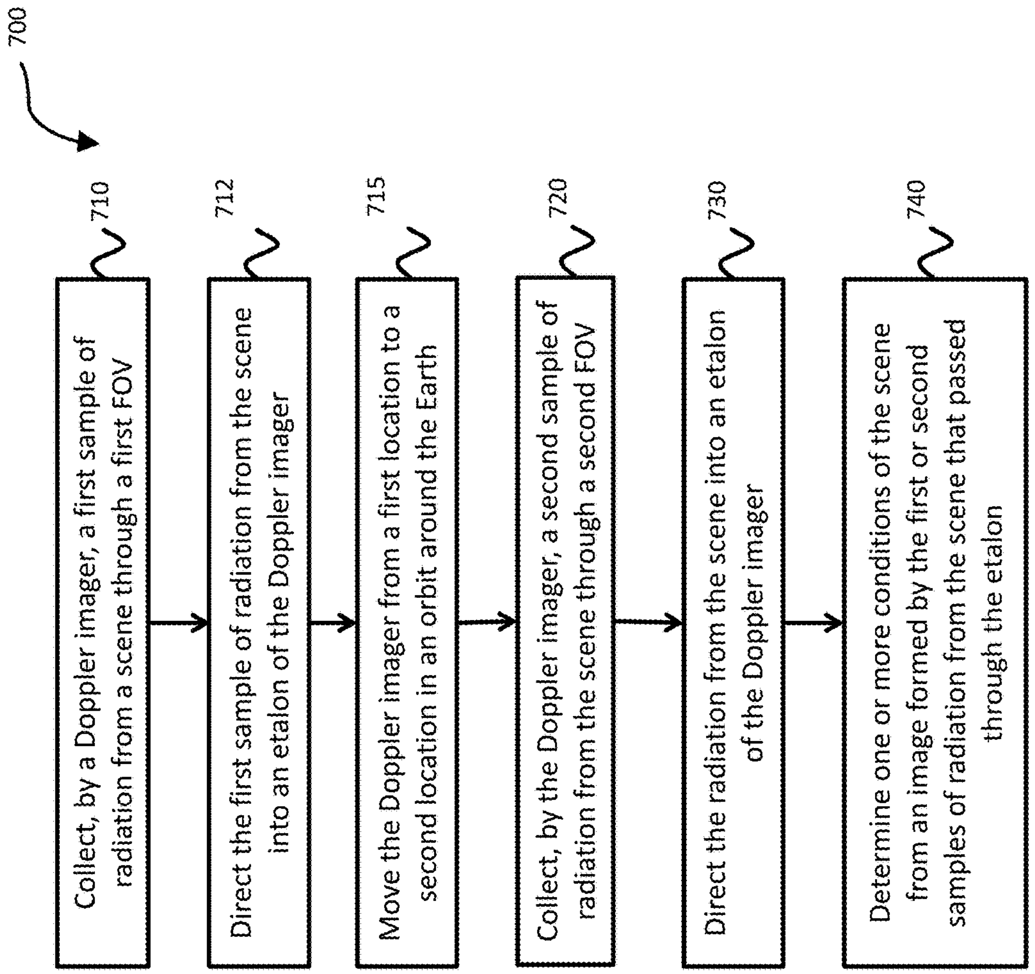
700
710
Collect, by a Doppler imager, a first sample of radiation from a scene through a first FOV
712
Direct the first sample of radiation from the scene into an etalon of the Doppler imager
715
Move the Doppler imager from a first location to a second location in an orbit around the Earth
720
Collect, by the Doppler imager, a second sample of radiation from the scene through a second FOV
730
Direct the radiation from the scene into an etalon of the Doppler imager
740
Determine one or more conditions of the scene from an image formed by the first or second samples of radiation from the scene that passed through the etalon

FIG. 7

SPLIT FIELD SPECTRAL IMAGER

PRIORITY CLAIM

The present Application for Patent claims priority to U.S. Provisional Patent Application No. 61/846,986 by Marchant et al., entitled "Split Field Spectral Imager," filed Jul. 16, 2013, assigned to the assignee hereof, and expressly incorporated by reference herein.

TECHNICAL FIELD

The present disclosure relates to optical spectroscopy, and more specifically to devices and methods for spectral imaging. Spectral imaging may refer to collecting and analyzing radiation from a scene in order to create a spatially resolved characterization of electromagnetic spectral content of the scene. The present disclosure relates to devices and methods for detecting spatial Doppler shifting of electromagnetic radiation that may be the result of the behavior or conditions of a target surface or an intermediate medium, such as an atmosphere or a liquid or gaseous volume.

SUMMARY

The following specification relates to methods, apparatuses and improvements in spectroscopy and Doppler imaging. Weather models and measurements play a critical role in shipping itineraries, private and commercial transportation, regional emergency preparedness, aerospace and many other endeavors. Accuracy and precision of weather forecasts depend on the computational details of the weather models and the accuracy and detail of observational initialization data. The vast majority of meteorological data recorded is taken from the lowest layers of the atmosphere, where in situ sensors are practical and relatively inexpensive. Because the upper layers of the atmosphere are difficult to directly measure with traditional barometric pressure sensors, thermometers and wind sensors, the upper layers have not been observed to the same degree as the lower layers.

In one configuration, a Doppler imager is described. The Doppler imager may include fore-optics configured to collect radiation from two or more fields of view and intermediate optics configured to superimpose the radiation into a composite intermediate image. The Doppler imager may also include a Fabry-Perot etalon configured to spatially modulate the composite image into a modulated image. The Doppler imager may further include aft-optics configured to focus the modulated image onto non-overlapping regions of a focal plane array.

In another configuration, a method for Doppler imaging is described. The method may include collecting, by a Doppler imager, radiation from a medium along a first field of view and along a second field of view. The method may also include directing the radiation into an etalon of the Doppler imager. The method may further include determining one or more conditions of the medium from an image of the radiation that passed through the etalon.

BRIEF DESCRIPTION OF THE DRAWINGS

FIG. **1** illustrates one embodiment of a split-field Doppler imager;

FIG. **2** illustrates one embodiment of a Fabry-Perot etalon and its function;

FIG. **3** illustrates another embodiment of a Fabry-Perot etalon;

FIG. **4** illustrates spectral changes of a known radiation source due to a Doppler shift;

FIG. **5** is an example of an image collected by a split-field Doppler imaging device;

FIG. **6** is a schematic drawing illustrating one application of a satellite-based split-field Doppler imaging device; and

FIG. **7** is a flowchart illustrating an example method of Doppler imaging.

DETAILED DESCRIPTION

The present disclosure covers apparatuses and associated methods for split-field Doppler imaging. In the following description, numerous specific details are provided for a thorough understanding of specific embodiments. However, those skilled in the art will recognize that embodiments can be practiced without one or more of the specific details, or with other methods, components, materials, and the like. In some cases, well-known structures, materials, or operations are not shown or described in detail in order to avoid obscuring aspects of the embodiments. Furthermore, the described features, structures, or characteristics may be combined in any suitable manner in a variety of alternative embodiments. Thus, the following more detailed description of the embodiments of the present disclosure, as illustrated in some aspects in the drawings, is not intended to limit the scope of the disclosure but is merely representative of the various embodiments of the disclosure.

In this specification and the claims that follow, singular forms such as "a," "an," and "the" include plural forms unless the content clearly dictates otherwise. All ranges disclosed herein include, unless specifically indicated, all endpoints and intermediate values. In addition, "optional," "optionally," or "or" refer, for example, to instances in which subsequently described circumstance may or may not occur, and include instances in which the circumstance occurs and instances in which the circumstance does not occur. The terms "one or more" and "at least one" refer, for example, to instances in which one of the subsequently described circumstances occurs, and to instances in which more than one of the subsequently described circumstances occurs.

The following specification relates to methods, apparatuses and improvements in spectroscopy and Doppler imaging. Weather models and measurements play a critical role in shipping itineraries, private and commercial transportation, regional emergency preparedness, aerospace and many other endeavors. Accuracy and precision of weather forecasts depend on the computational details of the weather models and the accuracy and detail of observational initialization data. The vast majority of meteorological data recorded is taken from the lowest layers of the atmosphere, where in situ sensors are practical and relatively inexpensive. Because the upper layers of the atmosphere are difficult to directly measure with traditional barometric pressure sensors, thermometers and wind sensors, the upper layers have not been observed to the same degree as the lower layers.

Some more primitive weather models may virtually exclude contributions and effects of the upper layers of the atmosphere and thus are unable to account for its changes and influence. Increasing data accumulated from the upper atmosphere may aid in creating more accurate weather models and may improve the accuracy and precision of weather forecasts. In the past several decades, researchers have employed Doppler-sensing instruments in order to remotely observe temperature, barometric pressure, wind speed, and wind direction of higher layers of the atmosphere. Doppler Sensing may refer to detecting spectral content and behavior from one or more directions in order to infer temperature and wind motion of molecules or particles in a region of interest.

Doppler Sensing can be used to acquire a spatially resolved image of Doppler shifts in an electromagnetic emission or absorption spectrum within one or more fields of view. Spatial resolution may be used in matching meteorological phenomena to geographic position, further enhancing the detail and precision of meteorological data acquired. When operating a Doppler imaging device to observe conditions of the upper atmosphere, it may be advantageous to deploy the device on an aircraft or satellite in order to avoid interference or back scattering from clouds or other particles prevalent in the lower layers of the atmosphere. Bulky and complex Doppler imaging apparatuses are not ideal for operation on a satellite because of size, mass and power restrictions and the fact that satellites are not readily accessible for repairs. For example, an active Doppler Sensor includes an illumination source that greatly increases the sensor size and power. For the forgoing reasons, the researchers of the present disclosure have identified a need for a static (e.g., no moving parts), passive (e.g., no illuminator), compact, and/or robust Doppler imaging apparatus capable of acquiring spatially resolved images of high-resolution Doppler data from a scene.

Doppler sensing methods analyze the wavelength shift and spectrum of a known light source traveling through a medium of interest in order to infer conditions or behavior of the medium. The medium may be an atmosphere comprising gasses and particulate matter, and the conditions of that medium may be temperature, barometric pressure, wind speed, or wind direction. Well-defined electromagnetic radiation from a known source may pass through the atmosphere and interact with gas molecules and other particles via scattering, luminescence, reflection, emission, or absorption. The known source could be radiation from an atomic or molecular event, such as an electron transition or chemical transition in atmospheric gasses. Atoms, molecules or particles in the medium may absorb photons of an original wavelength and re-emit photons having a shifted wavelength. Alternatively, the known source may be atomic or molecular events within the medium emitting photons with wavelength shifted from a nominal value. The shift in wavelength may depend on the velocity of the atom, molecule or particle with respect to an observer. Shifts in the mean wavelength may be referred to as "red-shifts" or "blue-shifts," depending on the direction of movement of the molecule or particle with respect to the observer. Atoms, molecules or particles re-emitting photons while traveling toward an observer will emit a blue-shifted photon (shorter wavelength), while atoms, molecules or particles traveling away from an observer will emit a red-shifted photon (longer wavelength). A statistical distribution of wavelengths absorbed or emitted may also depend on intrinsic properties of the medium, including temperature and pressure.

If many photons are measured or analyzed, one may obtain a detailed wavelength distribution or spectrum. Details of the spectrum, such as line width, may be due to the behavior of molecules or particles in an intermediary medium. By comparison with the known source spectrum or with reference to a physical model of the light source, the shift or shape of the spectrum can provide information about the general behavior or state of the medium, which includes but is not limited to temperature, wind speeds, wind direction, and barometric pressure.

One can retrieve spatially resolved spectral data using a Fabry-Perot etalon with a known etalon transmission function in an optical system with the following characteristics. Each resolved region of the scene illuminates corresponding non-overlapping areas on the image plane through the etalon; each point on the image plane area is illuminated predominantly by rays that pass through the etalon at approximately the same angle of incidence; and the image plane area includes at least one fringe of the etalon interferogram. Spectral information for the resolved region of the scene may be obtained by analyzing one or more of the location, width, and profile of the observed fringes with reference to the etalon's known transmission function.

Alternatively, one can retrieve spatially resolved spectral data using a Fabry-Perot etalon with a known etalon transmission function in an optical system with the following characteristics. The scene is imaged onto an image plane through the etalon; the optical rays from each point in the scene pass through the etalon at approximately the same angle of incidence; and multiple images are collected while scanning the optical system such that a target point in the scene passes through at least one fringe of the etalon interferogram. The spectral information for the target point may be obtained by constructing a fringe pattern corresponding to the target point as observed in the multiple images and analyzing the location, width, and profile of the observed fringes with reference to the etalon's known transmission function.

Fabry-Perot etalons have the advantage of a compact design and may function with no moving parts, providing added robustness to a system. The operation of a Fabry-Perot etalon and its interferogram fringe pattern will be discussed herein.

Observing light from a scene from two or more non-parallel directions may be beneficial in uniquely ascertaining a two-dimensional wind direction using a Doppler Sensor. The spectra of a scene imaged from two different directions can be compared against one another in order to infer wind directions by position in the scene. By measuring the spectrum of a single scene from two or more non-parallel directions, more accurate and precise inferences can be made about the temperature, wind speed, etc. of the atmosphere or medium.

Imaging a scene from two directions may be performed using duplicate light sensors working in harmony to record a single measurement. Duplicate components can decrease performance efficiency and increase manufacturing expense. Collecting images from two or more scenes simultaneously and projecting the images onto distinct sectors of a single focal plane array may maintain operational efficiency and a low-cost design. This method may be referred to as split-field imaging. In embodiments, a Doppler split-field imager is configured to collect light from two or more non-parallel directions and project the light from the multiple directions through a Fabry-Perot etalon and subsequently onto separate sectors of a single focal plane array. Split-field imaging may refer to a method of focusing light from multiple non-parallel fields of view onto a single focal plane array without image overlap. If the sensor is moving, multiple views of a single scene may be constructed by combining split-field sectors from two or more successive images.

FIG. **1** is a schematic drawing illustrating one embodiment of a split-field Doppler imaging apparatus **10**. FIG. **1** shows radiation **105** entering through a single aperture **110***a*, which may be referred to as a forward aperture **110***a*. The drawing illustrates two apertures, the forward aperture **110***a* and an aft aperture **110***b*. Radiation **105** may also enter through the aft aperture **110***b*. However, in order to preserve the visual simplicity of the drawing, FIG. **1** shows ray tracing only along a path of the radiation **105** entering the forward aperture **110***a*. In this example, the two apertures, **110***a* and **110***b*, are oriented to collect radiation **105** from non-overlapping fields of view. Radiation **105** entering through the forward aperture **110***a* and aft aperture **110***b* reflects off mirrors **115***a* and **115***b*, respectively. Light reflecting off either of the two mirrors **115***a* and **115***b* may then reflect off a surface of a field splitter **120** configured to superimpose the forward and aft radiation **105** onto a single composite intermediate image plane near the apex of the field splitter **120**. Subsequently, the superimposed radiation **105** reflects off a mirror **130** configured to direct radiation **105** through a Fabry-Perot etalon **150**.

Some embodiments of a split-field Doppler imaging apparatus **10** may also include collimating optics **152** which comprise one or more lenses or mirrors configured to collimate light rays from each point in the composite image prior to passage through the Fabry-Perot etalon **150**. Additionally, one or more re-imaging lenses or mirrors **175** positioned optically after the Fabry-Perot etalon **150** may be configured to refocus the light rays from each point in the composite image onto a point on the focal plane array.

The radiation **105** that passes through the etalon **150** may be spatially modulated with respect to the transmission function of the etalon **150**, which may be dependent on the thickness of an etalon gap **155**, an index of refraction of etalon gap **155**, an internal angle of incidence of the radiation **105** entering etalon **150**, and wavelength of the radiation **105**. The radiation **105** may then pass through a band-pass filter **170** configured to confine the wavelengths of the radiation **105** that are focused onto a focal plane array (FPA) or camera **180** by a re-imaging lens **175**.

Furthermore, in some examples of the imaging apparatus **10**, a calibration source **160** may be positioned to illuminate the focal plane through the etalon **150**. The calibration source **160** may emit a known spectrum of radiation that is conditioned by the etalon **150** and focused onto the FPA **180** to aid in calibrating the imaging apparatus **10**. During calibration of imaging apparatus **10**, imaging apparatus **10** may be configured such that the only radiation impinging on the FPA **180** is radiation supplied by the calibration source **160**. In some embodiments, calibrating the imaging apparatus **10** may be a step that is routinely and frequently executed in order to provide more accurate and precise spectral measurements of a scene.

Referring to FIG. **2**, a Fabry-Perot etalon **150** may be briefly described as an optical filter with two parallel, partially reflecting surfaces and no moving parts. A transmission function of an etalon describes a fraction of energy in a light ray that is transmitted through the etalon. The transmission function, $T(\lambda,d)$, of the etalon may be a function of wavelength of the ray λ, and an effective etalon path length d through the etalon. The effective etalon path length $d(\lambda,\theta)$ may be a function of an etalon gap spacing d_0 **155** between the two partially reflecting surfaces, the index of refraction n of the etalon gap material, and the angle of incidence of the light ray θ entering the etalon **150**. For example, in FIG. **2** an angle of incidence for ray **211** is denoted by θ_1 **215** while an angle of incidence for parallel rays **221** and **231** is denoted by θ_2 **225**.

The transmission function demonstrates that the transmission of a ray of energy through a Fabry-Perot etalon depends on the wavelength of the ray and the effective etalon path length. A ray of light having one combination of wavelength and angle of incidence may exit the etalon with little attenuation, while a ray having a different combination of wavelength and angle of incidence may be reflected and/or absorbed with strong transmissive attenuation. The result of the transmission function of the etalon on monochromatic incoming energy may be a pattern of concentric interference fringes or rings referred to as an interferogram that, when analyzed, can provide spectral information about the scene.

FIG. **2** is a schematic drawing illustrating the coherent transmission and attenuation of electromagnetic energy through a Fabry-Perot etalon **150**. A first incoming ray **211** with an angle of incidence θ_1 **215**, an initial phase ϕ_0 (not illustrated) and a wavelength λ_1 **217**, passes through a first partially reflective surface **133** and enters the etalon gap **155**. The first ray **211** then reflects off a second partially reflective surface **137**, which is parallel to the first partially reflective surface **133**. The first ray **211** reflects off the first partially reflective surface **133**. The first ray **211** may maintain the same angle of incidence with respect to the partially reflective surfaces **133** and **137**. The coherent radiation, giving rise to ray **211**, may be understood as a succession of planar wavefronts. This radiation gives rise to other rays parallel to ray **211**, including ray **212** that enters the etalon with phase ϕ_1 at the point where ray **211** is reflected from surface **133**. The combination of λ_1 and effective etalon thickness $d(\lambda_1, \theta_1)$ are such that the phase of ray **211** as reflected from surface **133** also equals ϕ_1. Because ray **212** has the same phase ϕ_1 as the reflected first ray **211** inside the etalon **150**, the first ray **211** and second ray **212** are considered to be in phase and undergo constructive interference **210**, whereby transmission of the electromagnetic energy through the etalon **150** is enhanced and its reflection and attenuation are minimized.

A third ray **221** has the same wavelength λ_1 as the first **211** and second **212** rays, but a different angle of incidence θ_2 **225**. Similar to the first ray **211**, the third ray **221** passes through the first reflective surface **133** with phase ϕ_3 and reflects off the second reflective surface **137**. The third ray reflects off the first reflective surface **133**, maintaining the same wavelength λ_1 **217** and angle of incidence θ_2 **225**. A fourth ray **222** arising from the same coherent radiation as ray **221** has the same wavelength **217** and angle of incidence θ_2 **225** as the third ray **221**. The fourth ray **222** passes through the first partially reflective surface **133** with phase ϕ_4 at the location where the third ray **221** reflects off the first partially reflective surface **133**. The combination of λ_1 and effective etalon thickness $d(\lambda_1,\theta_2)$ are such that the phase of the third ray **221** as reflected from surface **133** differs from ϕ_4 by 180 degrees. Because the fourth ray **222** is out of phase with the third ray **221**, the third ray **221** and fourth ray **222** may undergo deconstructive interference **220** whereby reflection and attenuation of the electromagnetic energy is maximized and its transmission through the etalon **150** is minimized.

A fifth ray **231** with wavelength λ_2 **227**, angle of incidence θ_2 **225** and phase ϕ_5 passes through the first partially reflective surface **133**. Like the first ray **211** and third ray **221**, the fifth ray **231** reflects off the second partially reflective surface **137** and off the first partially reflective surface **133**. A sixth ray **232** arising from the same coherent radiation as the fifth ray **231** passes through the first partially reflective surface **133** with phase ϕ_6 at the location where the fifth ray **231** reflects off the first partially reflective surface **133**. The combination of λ_2 and effective etalon thickness $d(\lambda_2,\theta_2)$ are such that the phase of the fifth ray **231** as reflected from the first partially reflective surface **133** matches ϕ_6. The two interfering rays **231** and **232** are in phase and undergo constructive interference **230** whereby transmission of the electromagnetic energy through the etalon **150** is maximized.

Although FIG. **2** illustrates multiple mutually coherent rays interfering, it should also be understood that the Fabry-Perot etalon **150** superimposes many rays, including contributions from higher-order reflections inside the etalon **150**. A purpose of FIG. **2** may be to illustrate how the transmission function of the etalon, T(λ,d), may be enhanced or reduced by interference effects within the etalon gap. Knowledge of T(λ,d) enables an analyst to derive information on the incoming radiation spectrum from images collected at the focal plane, such information including line-of-sight Doppler shifts due to behavior of a medium, such as temperature and wind.

FIG. **3** illustrates an alternate embodiment of a Fabry-Perot etalon **330**. While the design or manufacture of the embodiments may differ, the function may be essentially the same. Embodiments of a Fabry-Perot etalon described in this specification thus far may benefit from being able to function with no moving parts. In particular, the Fabry-Perot etalon **330** can function without any changes in the etalon gap thickness. In one embodiment, the Fabry-Perot etalon **330** comprises a single piece of glass or similar material with two parallel and opposing external surfaces **333** and **337**. The two parallel and opposing external surfaces **333** and **337** may be partially reflective. Similar to other embodiments, these partially reflective surfaces **333** and **337** may have reflection coefficients greater than 0 and less than 1. In some embodiments, reflective coefficients of the two external surfaces **333** and **337** may be the same or different. The opposing external surfaces **333** and **337** enclosing an etalon gap **335**, d_0, may be substantially parallel and that parallelism may be maintained by the structural integrity of the solid material comprising the etalon gap **335**. Embodiments similar to the etalon **330** described in FIG. **3** may have manufacturing or durability advantages.

As exemplified in FIG. **1**, one embodiment of a Fabry-Perot etalon **150** may comprise two pieces of glass or similar material, being separated by an etalon gap **155**. The etalon gap **155** may comprise a vacuum, gas, or some other material. The etalon gap **155** may have a different index of refraction than the two pieces of glass. The inside surfaces of the glass pieces may have partially reflective surfaces where each reflective surface may have the same or different reflectivity. The reflectivity R of the two surfaces may be greater than 0 and less than 1. In embodiments, the opposing reflective internal surfaces are parallel to one another. Furthermore, increasing or decreasing the reflectivity of the two surfaces may directly affect a coefficient of finesse F of the etalon **150**. The coefficient of finesse F may affect the appearance or structure of the interferogram. In embodiments where the etalon **150** has a relatively high coefficient of finesse F, the resulting interference fringes or rings may be narrower or more defined with respect to the spacing between successive fringes. Narrow or more defined fringes may be easier to discern and analyze, and may provide more precise measurements while broader, brighter fringes from an etalon with a relatively small coefficient of finesse F may be beneficial in situations with less incoming energy. The coefficient of finesse F may be entirely dependent on the reflectivity and may be defined by the relationship:

$$F = \frac{4R}{(1-R)^2}$$

where R is the reflectivity.

Returning to FIG. **3**, incoming radiant energy **310** may have varying angles of incidence. However, it may be advantageous that the angles of incidence are confined to be relatively small or near normal (between 0 to 10 degrees). Confining the field of view of the scanning etalon spectroscopy device to near-normal angles of incidence may limit the number of interference rings produced by the etalon, which may allow for simpler, faster, or more precise data analysis.

FIG. **4** is a graph illustrating spectral changes of a known radiation source due to a Doppler shift. In particular, FIG. **4** demonstrates a Doppler broadening of a reference spectrum due to thermal behavior of an emitting or scattering medium. A narrower Lorentzian curve **410** shown represents a reference emission spectrum in the absence of Doppler broadening. In some cases, a known source that provides the reference emission spectrum may be the result of some atomic emission event, such as electron transitions of atomic oxygen in the upper atmosphere. Such atomic emission events may occur more frequently in higher regions of the atmosphere, a convenient phenomenon that provides an altitude-specific source of radiation.

Referring to FIG. **4**, the taller, narrower peak **410** shows the pure original source of radiation, e.g., from isolated atoms at rest, while the shorter, broader, Gaussian peak **420** shows a modified spectrum emitted from a thermalized ensemble of emitters or radiation scattered by a medium including thermalized atoms or molecules. Atoms or molecules in the medium may absorb photons of the pure and well-known radiation source and reemit the photons while in motion. The reemitted photons may have slightly shifted wavelengths depending on a velocity of the molecule or particle during reemission with respect to an observer. When many of the reemitted photons are collected and analyzed, a spectrum **420** can be measured. The measured spectrum **420** of the Doppler-shifted light has a broader range and a shallower peak due to the Doppler shifting within the medium.

The Lorentzian **410** and Gaussian **420** spectra in FIG. **4** may have peaks located at the same position along the horizontal axis. The horizontal axis represents wavelength and the vertical axis represents amplitude. In this case, it may be inferred that the Doppler shifting that occurred was due entirely to the temperature of the medium, and not due to bulk motion or wind. In cases where wind is responsible for the Doppler shifting of radiation, the peak or mean value of the Gaussian spectrum **420** may be expected to shift along the wavelength axis depending on the direction and speed of the wind with respect to the Doppler imaging device. If a wind vector in a field of view has a substantial component heading towards the Doppler imager (e.g., observer), then there will be an overall trend of blue shifting, and the peak would shift to the left along the wavelength axis. If a substantial component of the wind vector is heading away from the Doppler imager, then there will be an overall trend of red shifting of the imaged medium, and the peak would move to the right along the wavelength axis.

FIG. **5** is an example of a single prophetic image captured by a split-field Doppler imaging device using a Fabry-Perot etalon, such as split-field Doppler imaging device **10** of FIG. **1** using the Fabry-Perot etalon **150** or **330** of FIGS. **2** and **3**, respectively. If the Doppler imaging device **10** were to be used on a satellite, the source of energy may be a scene from the atmosphere or surface of the Earth. FIG. **5** shows two scenes that may be simultaneously imaged by the Doppler imaging device **10**. The two scenes may be imaged on a single Focal Plane Array, with the Doppler imaging device **10** configured to image a scene from two different points of reference as the device moves with respect to the scene. The image shows transmission fringes from an interferogram from the etalon spatially modulating an image of the scene. The image is split down the center, with a left side **510** imaging a first scene and a right side **520** imaging a second scene. The interferogram is also split, and has subtle but measurable differences in fringe phase and spacing on the two sides **510** and **520**. This may be due to slightly different spectral content from the two scenes, which when modulated by the interferogram, produces differences in the interferogram's pattern or structure. A scene may scan across the field of view of the Doppler imaging device **10**, or vice versa, while the Doppler imaging device **10** takes several consecutive images. The image of the moving scene may be said to modulate the interferogram. The interferogram of each image can be analyzed and deconvolved with respect to the etalon transmission function in order to determine at least one characteristic about the scene spectrum.

A Doppler imaging device that does not have split-field capabilities may be able to detect only changes in wavelength due to line-of-sight Doppler shifts between an emission or scattering event and an observer. Thus, one cannot accurately characterize the wind vectors if the scene were only measured from one direction. By measuring a single scene, such as a region on the surface of the earth, from at least two non-parallel directions, one could compare the two or more line of sight Doppler shifts of the scene from the plurality of directions in order to correctly characterize the direction of the wind. If a split-field spectral imager, such as split-field Doppler imaging device **10**, were to be used on a satellite, the device **10** may image a region of the Earth from two directions by imaging the region at a first time from a forward aperture, and later image the same scene at a second time through the aft aperture. In this application, one must assume that the local wind vector is the same during the Forward and Aft image captures.

FIG. **6** is a schematic drawing illustrating an operational deployment of a split-field Doppler imaging device, such as split-field Doppler imaging device **10** of FIG. **1**. FIG. **6** shows a satellite **610** in an orbit **630** around the Earth **650**. The satellite **610** is outfitted with a split-field Doppler imaging device **10**, which collects incoming radiation from the Earth's atmosphere **640** in two fields of view (FOV) **620***a* and **620***b* and projects focused radiation from the two field of views onto a single image plane within the device **10**. One field of view may be referred to as the "Forward FOV" **620***a* while the other may be referred to as the "Aft FOV" **620***b*. With reference to FIG. **6**, one may see that as the satellite **610** moves in an orbit **630** around the earth **650**, a scene first captured in the Forward FOV **620***a* may eventually be re-captured, at least in part, by the Aft FOV **620***b*. Referring back to FIG. **5**, the left side **510***b* may show a scene from the Aft FOV **620***b*, while the right side **510***a* of the image may show a scene captured in the Forward FOV **620***a*.

Because the scene brightness from the Earth's atmosphere may be low, it may be advantageous to incorporate in the instrument a high-sensitivity FPA. For example, the FPA may be an electron-multiplied charge coupled device (EM-CCD) that is sensitive to signal differences as small as a single photoelectron.

To further explain how a wind vector can be characterized from imaging a scene from two non-parallel directions, consider a horizontal wind field **645** moving uniformly towards the left in FIG. **6** above the Earth's surface along the orbital direction of the satellite **610**. If the satellite **610** were stationary in the location as drawn, the photons collected by the split-field Doppler imaging device **10** in the Forward field of view would be blue shifted, while the photons collected in the Aft field of view would be red shifted. By comparing these two shifted spectrums, the line of sight Doppler shift components can be aggregated and compared to yield a horizontal wind vector (direction and magnitude) for each point in the scene. In practice, the satellite **610** is moving along its orbit **630** with a substantial and accurately known orbital velocity. This adds a blue shift to the Doppler observation of the Forward FOV and a red shift to the Doppler observation of the Aft FOV. The known satellite velocity is then subtracted from the derived relative wind vector to obtain the wind field vector **645** relative to the Earth.

In operation, a scanning etalon spectroscopic imaging device like those shown in FIGS. **1** and **6** may be positioned or configured to scan a scene comprising a field of view where the scene may emit radiant energy at one or more frequencies. In one example, we may consider using split-field Doppler imaging device to detect wind vectors and temperature in the upper layers of the Earth's atmosphere.

First, a spectral band for some electromagnetic emission or scattering event in the upper atmosphere is selected. This spectral band may be an emission line for atomic Oxygen, which is most abundant in the upper atmosphere. The emission line of atomic Oxygen may be represented as one or more narrow peaks, having a well-known and defined spectral profile. For example, the diatomic oxygen atmospheric band (A-band) consists of two major peaks near 762 nm.

A calibration image may be collected of a uniform monochromatic scene for which the wavelength is precisely known. The calibration image may then be analyzed and precise geometrical and optical characteristics of the etalon may be derived. The characteristics may comprise the centration of the interferogram pattern on the focal plane. The centration may refer to the geometrical center of the interferogram, which may comprise a series of concentric fringes. The characteristics may further comprise an effective focal length of the reimaging lens **170**, and the image distortion due to the reimaging lens **170**, which may be due to the detailed structure of the lens. Distortions or aberrations caused by imaging lenses may modify the ideal shape of the image or interferogram, leading to inaccurate calculations if not corrected. Distortion may be accounted for in image analysis, or may be corrected using corrective optics. The derived optical characteristics may further comprise etalon cavity thickness, which may depend on the etalon gap **155**, the index of refraction of the material in the etalon gap **155**, and the angle of incidence of the energy upon entering the etalon **150**. The derived optical characteristics may further comprise an etalon coefficient of finesse F, which may depend on the reflectivity of the two reflective surfaces of the etalon, where a high reflectivity (e.g. 0.75-0.99) may result in a high coefficient of finesse F.

An effective thickness of the etalon **150** or **330** may then be calculated for each pixel on the FPA **180**. As stated earlier, the effective etalon thickness may depend on the angle of incidence of radiant energy **110**, where the angle of incidence of incoming energy **110** may be matched to a points or pixels on the image plane, or FPA **180**. The effective etalon thickness at each pixel, or d_i, where the subscript "i" denotes the pixel number, may be calculated by the function:

$$d_i = n \cdot d_0 \cdot \cos\theta_i$$

where d_0 represents the etalon gap thickness and θ_i represents the internal angle of incidence of rays of energy **110** on the reflective etalon surfaces. For the case n=1, the internal angle of incidence is equal to the angle of incidence for radiation entering the etalon. Otherwise the internal angle of incidence depends on the external angle of incidence and the value of n in accordance with Snell's Law. The transmission of radiation **110** passing through the etalon **150** may be a function of wavelength λ and effective etalon thickness d. The transmission function may have the form:

$$T(\lambda, d) = \frac{1}{1 + F \cdot \sin^2(\delta)} \text{ where } \delta = \frac{2\pi d}{\lambda}.$$

After collecting one or more calibration images, a series of images may be collected as the scene scans across the field of view of the device, or vice versa. The images may be calibrated to remove pixel offsets such as readout bias or dark current. The images may also be corrected for pixel-to-pixel variations in the readout gain and response non-linearity. Then, combining the calibrated pixel values for a scene point in each image, a function $S_p(d)$ of signal versus effective etalon thickness (d), may be constructed. The subscript "p" in the Signal function $S_p(d)$ may denote the signal at a given scene point referred to as "p." Similarly, the subscript "p" may also denote the pixel for which the signal is calculated. Each point in a scene may correspond to a given pixel on the focal plane array.

Alternatively, if the spatially resolved target point p covers multiple pixels at the image, the function $S_p(d)$ may be constructed from the signal values of a single image without scanning of the scene.

The signal function of a point p in a scene may be an integral of the scene spectral radiance $L_p(\lambda)$ and the transmission of the etalon $T(\lambda,d)$ over the bandpass of the sensor, where the bandpass of the sensor may refer to the range of wavelengths observed or collected by the sensor. The signal function may be defined as:

$$S_p(d) = \int_{bandpass} d\lambda \cdot T(\lambda, d) \cdot L_p(\lambda)$$

In matrix form, the above relationship may also be written as:

$$S_d = T_{d\lambda} \cdot L_\lambda$$

The signal function S_p must account for separate regions of the focal plane array. In some embodiments, the focal plane array may be divided into two regions, each region being illuminated by radiation from either a forward or an aft aperture, as illustrated in FIG. **5**. This fact may become significant during spectroscopic analysis. In some embodiments, there may be a time offset between forward and aft images of a scene on the Earth or other observed body. By knowing the velocity of the orbiting satellite with respect to the Earth, the forward and aft images of a scene can be matched and analyzed in order to calculate wind vectors for each point in a scene.

If the number of independent image values in S_d equals the number of wavelength values in the spectrum (size of L_λ), then the relationship for Signal S_d to Transmission $T_{d\lambda}$ and Spectral Radiance L_λ may be solved for L_λ to give:

$$L_\lambda = T_{d\lambda}^{-1} \cdot S_d$$

If the size of S_d exceeds the size of L_λ, then a fit to the spectrum may be approximated for example using the pseudo-inverse method:

$$L_\lambda = (T^T \cdot T)^{-1} \cdot T^T \cdot S_d$$

Note that no unique solution is possible if the size of S_d is less than the number of wavelengths.

FIG. **7** is a flowchart illustrating an example method **700** of Doppler imaging. For clarity, the method **700** may apply to aspects of the split-field Doppler imaging device **10** described with reference to FIG. **1** or aspects of one or more of the Fabry-Perot etalons **150** and **330** described with reference to FIG. **1**, **2**, or **3**. In some examples, the Doppler imaging is split-field Doppler imaging.

At block **710**, the method **700** may include collecting, by a Doppler imager, a first sample of radiation from a scene through a first field of view. The operation(s) at block **710** may be performed using the forward aperture **110***a* described with reference to the split-field Doppler imaging device **10** of FIG. **1**.

At block **712**, the method **700** may also include directing the first sample of radiation from the scene into an etalon of the Doppler imager. For example, the radiation **105** may be directed through the Doppler imager to be incident upon the etalon **150** one or more of the Fabry-Perot etalons **150** and **330** described with reference to FIG. **1**, **2**, or **3**. The etalon **150** may include an etalon gap that comprises a space or a solid material, such as the etalon gap **155** of FIGS. **1** and **2** and the etalon gap **335** of FIG. **3**. In some examples, the Doppler imager further includes intermediate optics configured to superimpose the radiation **105** into a composite intermediate image and to the etalon.

At block **715**, the method **700** may include moving the Doppler imager from a first location to a second location in an orbit around the Earth.

At block **720**, the method **700** may include collecting, by the Doppler imager, a second sample of radiation from the scene through a second field of view. The operation(s) at block **720** may be performed using the aft aperture **110***b* described with reference to the split-field Doppler imaging device **10** of FIG. **1**. In some examples, collecting the first sample of radiation through the first field of view further includes collecting the radiation from a first aperture along a first direction, wherein collecting the second sample of radiation through the second field of view further comprises collecting the radiation from a second aperture along a second direction, wherein the first direction is non-parallel with the second direction. For example, the forward aperture **110***a* collects the radiation **105** from a first FOV, such as FOV **620***a* of FIG. **6**. The aft aperture **110***b* collects the radiation **105** from a second FOV, such as FOV **620***b* of FIG. **6**.

At block **740**, the method **700** may further include determining one or more conditions of the scene from an image formed by the first or second samples of radiation that passed through the etalon. Examples of the one or more conditions of the scene include wind vectors or the temperature within the scene.

The method **700** may include collecting a calibration image of a uniform monochromatic scene of an event for which the wavelength of the event is known. The event may be, for example, an EM Emission or scattering event in the upper atmosphere of the Earth or another object. The method **700** may also include calibrating the Doppler imager based at least in part on the calibration image. The method **700** may include analyzing the calibration image and deriving precise geometrical or optical characteristics of the etalon. Examples of the geometrical and optical characteristics of the etalon include at least one of centration of an interferogram pattern of the image, an effective focal length of a reimaging lens of the Doppler imager, one or more distortions or aberrations caused by one or more imaging lenses of the Doppler imager, a cavity thickness of the etalon, an index of refraction of material in an etalon gap, an angle of incidence of the radiation upon entering the etalon, and an etalon coefficient of finesse F, or combinations thereof. Some further examples of method **700** include correcting for any distortions detected in the etalon.

The method **700** may further include creating a weather model based at least in part on the one or more conditions of the scene. The method **700** may further include determining a temperature, a bulk motion, or a wind of the medium. The method **700** may include determining a wind speed and direction based on Doppler shifting of a measured spectrum with a reference spectrum. For example, wherein the method may include taking a calibration image that comprises a reference spectrum and determining a Doppler shifting of the image based at least in part on a comparison of the image with the reference spectrum. From the determined Doppler shifting, the method **700** may include determining a wind vector of the medium based at least in part on the Doppler shifting. Some examples of method **700** include analyzing a Doppler broadening of a reference spectrum due to thermal behavior of an emitting or scattering medium.

In some examples, such as the satellite **610** example of FIG. **6**, the photons collected by the forward aperture **110***a* (forward field of view) may be blue shifted, while the photons collected in the collected by the aft aperture **110***b* (aft field of view) may be red shifted. The method **700** may further include comparing these two shifted spectrums, and comparing an aggregated line of sight Doppler shift components to yield a horizontal wind vector (direction and magnitude) for each point in the scene. In some examples, forward and aft measurements may be made at different times and the Doppler shifting may be analyzed with the assumption that the local wind vector is the same at the different times.

The method **700** may further include focusing the radiation that passed through the etalon onto an image plane area to generate the image, wherein each point on the image plane area is illuminated predominantly by the radiation that passed through the etalon at approximately the same angle of incidence. The Doppler imager may include aft-optics configured to focus the modulated image onto non-overlapping regions of a focal plane array.

In additional examples of method **700**, one or more additional images are collected to create a series of images. The series of images may be calibrated and corrected based at least in part on a calibration image. The one or more conditions of the medium may be determined from the series of images. For example, the interferogram of each image can be analyzed and deconvolved with respect to the etalon transmission function in order to determine at least one characteristic about the scene spectrum.

In some examples, the method **700** may confine the field of view of the scanning etalon spectroscopy device to near-normal angles of incidence. The method **700** may further limit the number of interference rings produced by the etalon, which may allow for simpler, faster, or more precise data analysis. In other examples, the method **700** may include matching a coefficient of finesse of the etalon to an expected intensity level of the incident radiation.

The above prescription yields the complete scene spectrum, which is readily exploited for scene characterization in many applications using many different analysis techniques. If the component target spectra are known a priori, the procedure detailed above may be modified so that the components of the L vector (a much reduced number) correspond to the several spectral components (not separate wavelengths per se) of the energy collected from the scene. The spectral radiance L can be compared with a known spectral radiance for some electromagnetic event in the upper atmosphere to infer changes in the spectrum due to the Doppler effect, and thereby to detect wind speeds and temperature.

What is claimed is:

1. A method of Doppler imaging, comprising:

collecting, by a Doppler imager, a first sample of radiation from a scene through a first field of view;

directing the first sample of radiation from the scene into an etalon of the Doppler imager;

moving the Doppler imager from a first location to a second location in an orbit around the Earth;

collecting, by the Doppler imager, a second sample of radiation from the scene through a second field of view;

directing the second sample of radiation from the scene into the etalon of the Doppler imager; and

determining one or more conditions of the scene from an image formed by the first or second samples of radiation from the scene that passed through the etalon;

wherein collecting the first sample of radiation from the scene through the first field of view further comprises collecting the radiation from a first aperture along a first direction, wherein collecting the second sample of radiation from the scene through the second field of view further comprises collecting the radiation from a second aperture along a second direction, wherein the first direction is non-parallel with the second direction.

2. The method of claim **1**, further comprising:

focusing the first and second samples of radiation that passed through the etalon onto an image plane area to generate the image, wherein each point on the image plane area is illuminated predominantly by the first and second samples of radiation that passed through the etalon at approximately the same angle of incidence.

3. The method of claim **1**, further comprising:

collecting a calibration image of a uniform monochromatic scene of an event for which the wavelength of the event is known.

4. The method of claim **3**, further comprising:

calibrating the Doppler imager based at least in part on the calibration image.

5. The method of claim **3**, wherein the calibration image comprises a reference spectrum, the method further comprising:

determining a Doppler shifting of the image based at least in part on a comparison of the image with the reference spectrum; and

determining a wind vector of the scene based at least in part on the Doppler shifting.

6. The method of claim **3**, further comprising:

deriving one or more geometrical or optical characteristics of the etalon from the image, wherein the one or more conditions of the etalon comprise at least one of:

centration of an interferogram pattern of the image,

an effective focal length of a reimaging lens of the Doppler imager,

one or more distortions or aberrations caused by one or more imaging lenses of the Doppler imager,

a cavity thickness of the etalon,

an index of refraction of material in an etalon gap,

an angle of incidence of the radiation upon entering the etalon, and

an etalon coefficient of finesse F,

or combinations thereof.

7. The method of claim **1**, wherein the image is a first image, the method further comprising:

collecting one or more additional images to create a series of images;

calibrating and correcting the series of images based at least in part on a calibration image; and

determining one or more conditions of the medium from the series of images.

8. The method of claim **1**, further comprising:

creating a weather model based at least in part on the one or more conditions of the scene.

9. The method of claim **1**, wherein the image is a modulated image, wherein the etalon comprises a Fabry-Perot etalon configured to spatially modulate a composite image into the modulated image, and wherein the Doppler imager comprises a split-field Doppler imaging device that further comprises intermediate optics configured to superimpose the radiation into a composite intermediate image and aft-optics configured to focus the modulated image onto non-overlapping regions of a focal plane array.

* * * * *